

**Preparation of respirable nanoparticle agglomerates of the low melting and ductile drug ibuprofen: impact of formulation parameters**

Maria Malamatari <sup>a</sup>, Satyanarayana Somavarapu <sup>a</sup>, Kyriakos Kachrimanis <sup>b</sup>,  
Graham Buckton <sup>a</sup>, Kevin MG Taylor <sup>a</sup>

<sup>a</sup> *UCL School of Pharmacy, 29-39 Brunswick Square, London, WC1N 1AX, UK*

<sup>b</sup> *Department of Pharmaceutical Technology, Faculty of Pharmacy, Aristotle University of Thessaloniki, 54124 Thessaloniki, Greece*

Corresponding authors:

Maria Malamatari and Kevin MG Taylor  
UCL School of Pharmacy,  
29-39 Brunswick Square,  
London, WC1N 1AX, UK

Email: [maria.malamatari.12@ucl.ac.uk](mailto:maria.malamatari.12@ucl.ac.uk) and [kevin.taylor@ucl.ac.uk](mailto:kevin.taylor@ucl.ac.uk)

Tel/Fax: +44 (0) 207 753 5853

## **ABSTRACT**

Ductile and low melting point drugs exhibit challenging behaviour during both particle size reduction and spray drying as considerable amount of heat is involved in both processes. In this study, a systematic approach was employed to understand the preparation and *in-vitro* performance of respirable nanoparticle agglomerates by coupling wet milling and spray drying for ibuprofen, which is a drug with a low melting point and challenging mechanical properties. Wet milling in the presence of two stabilizers differing in their thermal properties and subsequent spray drying of the suspensions were employed after the addition of mannitol and/or leucine. The effects of the stabilizer type and the amounts of mannitol (matrix former) and leucine (dispersibility enhancer), on the yield of the process, the particle size, the redispersibility (i.e. reformation of nanoparticles upon rehydration) and the aerosolization (fine particle fraction, FPF%) of the nanoparticle agglomerates were evaluated using standard least squares model and a 2<sup>3</sup> full factorial design (3 factors at 2 levels plus four centre points). All factors investigated were found to have a significant effect on the yield of nanoparticle agglomerates ( $p < 0.05$ ). The size of the nanoparticle agglomerates was mainly dependent on the leucine to drug ratio and the type of stabilizer ( $p < 0.05$ ), while mannitol to drug ratio was the only significant factor affecting the redispersibility of the formulations ( $p < 0.05$ ). The FPF%, determined using a fast screening impactor, was found to be dependent on both the leucine and mannitol to drug ratio ( $p < 0.05$ ). This study demonstrates the successful preparation of respirable nanoparticle agglomerates of low melting point and ductile ibuprofen and the usefulness of the design of experiments as a tool to understand the impact of the formulation parameters on their fabrication and *in-vitro* performance.

## 1     **1.     Introduction**

2

3     Nanocrystals are nanosized drug particles. Nanocrystals are typically produced in  
4     the form of nanosuspensions, which are submicron, colloidal dispersions of  
5     nanosized drug particles, stabilised by surfactants, polymers, or a mixture of both  
6     [1]. Nanocrystals have been suggested as a beneficial formulation approach for  
7     Class IIa drugs of the Biopharmaceutics Classification System (BCS), for which  
8     the dissolution rate is the rate-limiting step of absorption [2]. Considering the  
9     various nanosizing techniques (i.e. top-down and bottom-up), wet milling is a  
10    reproducible, cost-effective and scalable way of preparing nanosuspensions with  
11    a typical size ranging from 200-500 nm [3]. Wet milling is the technique for the  
12    preparation of the majority of the nanosuspension-based pharmaceutical  
13    formulations that are either on the market or currently under development [4,5].

14

15    Solidification of the nanosuspensions has been explored to combine the  
16    advantages of liquid nanosuspensions (i.e. enhanced dissolution and solubility)  
17    with the benefits of solid formulations (i.e. stability, easier handling, enhanced  
18    patient compliance) producing nanoparticle agglomerates suitable for oral and  
19    pulmonary delivery. Spray drying is a single-step process for the conversion of a  
20    liquid feed into a dried particulate form. It is a popular process from an industrial  
21    perspective as it is more cost- and time-effective compared to freeze drying [6].  
22    Therefore, preparation of nanosuspensions by wet milling followed by  
23    solidification, using spray drying, has been suggested as a formulation approach  
24    for nanoparticle agglomerates with enhanced dissolution and aerosolization  
25    efficiency [7–10].

26

27    Spray drying is also a fundamental particle engineering technique for pulmonary  
28    drug delivery due to its simplicity, adaptability and scalability. Spray drying is a  
29    rapid solidification procedure and the obtained particles (at least from solution  
30    feed) are usually amorphous. Amorphicity is regarded as a disadvantage for  
31    respirable particles as it is associated with the danger of recrystallisation upon  
32    storage, which may influence adversely the stability, dissolution, absorption and  
33    aerosolisation efficiency of the product [11]. Moreover, during spray drying  
34    nanocrystals are exposed to thermal stresses, which may cause irreversible

35 aggregation to the resultant formulations [12]. Irreversible aggregation is linked  
36 with poor redispersibility of the nanoparticle agglomerates, which cannot reform  
37 nanoparticles upon rehydration leading to the loss of the advantages of the  
38 nanoformulations [12,13].

39

40 Addition of generally recognised as safe (GRAS) excipients in the liquid feed  
41 before spray drying is a common strategy to manipulate the properties and thus the  
42 performance of the dry powders. Mannitol is a non-reducing sugar, which has been  
43 approved by regulatory authorities for use in inhalable pharmaceutical products  
44 [14]. In particular, mannitol exhibits excellent spray-drying properties as the size  
45 and morphology of the particles can be modified by varying the process parameters  
46 [15]. The crystallinity of the spray-dried mannitol and the non-hygroscopic nature  
47 of this excipient are advantageous for the long-term stability of the dry powders  
48 [16]. Moreover, mannitol has been used as a matrix former during the  
49 solidification of nanosuspensions [7,10,17–19]. As a water-soluble compound,  
50 mannitol forms a matrix around the nanoparticles, which upon rehydration  
51 dissolves allowing the reformation of the primary nanoparticles.

52

53 Leucine is an endogenous amino acid, which exhibits aerosolization-enhancing  
54 properties [14,16]. Leucine was found to influence particle formation and to  
55 reduce the cohesiveness of spray-dried mannitol particles, which subsequently  
56 resulted in higher emitted fractions [20,21]. According to Sou et al. [20], *“it is a  
57 combination of a high surface activity during the drying process, mass transport  
58 within the droplet, followed by subsequent self-assembly packing on the particle  
59 surface which may explain the dispersibility enhancing effect of leucine”*.  
60 Modification of particle morphology in response to higher concentrations of  
61 leucine has been previously reported [20,22]. More specifically, when leucine was  
62 co-spray dried with mannitol and trehalose it was found that a leucine  
63 concentration <5% w/w was insufficient for discrete particle formation, a  
64 concentration of 5-20% w/w resulted in reduced particle aggregation while a  
65 concentration >20% w/w led to increased surface corrugation [21]. According to  
66 Mangal et al. [23], the surface concentration of leucine governs particle formation  
67 and optimum surface concentration of this amino acid results in optimum surface  
68 and bulk properties of the spray-dried powders.

69 Ibuprofen was selected as a poorly water-soluble model drug with a low melting  
70 point (75-78 °C) and challenging mechanical properties as it exhibits a high brittle-  
71 ductile transition point of 854  $\mu\text{m}$  [24]. Below this point, it is hard to reduce the  
72 size of particles by dry milling, as the particles tend to deform rather than fragment.  
73 Despite the high ductility of ibuprofen, it was reported that wet milling using a  
74 Micros Ring Mill resulted in particles with a diameter about 8-11  $\mu\text{m}$  (much  
75 smaller than the critical diameter of 854  $\mu\text{m}$ ) [25]. The superior size reduction  
76 performance of wet milling was attributed to the contribution of shear forces,  
77 which cause ductile fracture of crystals. Besides the ductility of ibuprofen, its low  
78 melting point poses additional challenges to conventional nano-comminution  
79 techniques. The heat generated in the mill may result in partial melting of the drug  
80 particles and thereby formation of large aggregates or drug amorphisation [26–  
81 28]. In a recent study by Lestari et al. [29], ibuprofen was classified as a drug with  
82 poor millability as high concentrations of stabilizers and extended milling times  
83 were required to produce stable nanosuspensions by wet milling.

84

85 Ibuprofen is a nonsteroidal anti-inflammatory drug (NSAID) for treating fever,  
86 pain and inflammation; it was recently reported that ibuprofen acts synergistically  
87 with antibiotics and thus might play a multifunctional role in the treatment of  
88 cystic fibrosis infections [30]. Based on this new evidence, Yazdi et al. [31]  
89 formulated carrier-free dry powder inhalations of micronized (jet-milled)  
90 ibuprofen as an attractive alternative to oral administration of the drug in cystic  
91 fibrosis. Therefore, preparation of respirable nanoparticle agglomerates of  
92 ibuprofen with increased dissolution may be used as an alternative formulation  
93 approach for the targeted delivery of ibuprofen to the lungs.

94

95 In this study, wet milling of ibuprofen using two different stabilizers, namely  
96 hypromellose (HPMC) and D- $\alpha$ -tocopherol polyethylene glycol 1000 succinate  
97 (TPGS), followed by spray drying, after the addition of excipients, was assessed.  
98 Different grades of HPMCs have been found to be the most effective stabilizers  
99 in terms of particle size reduction and short-term physical stability of ibuprofen  
100 nanosuspensions [32] while TPGS due to its low viscosity and high surface  
101 activity has been identified as the surface modifier with the highest success rate  
102 on stabilizing nanosuspensions of various drugs [33]. These two stabilizers differ

103 with respect to their thermal properties; HPMC has a glass transition temperature  
104 of 125.5 °C [34] while TPGS is a thermosensitive surfactant with low melting  
105 point (m.p. 38 °C). The effect of these two stabilizers on the size reduction of  
106 nanosuspensions was investigated. The solid state, particle morphology and the  
107 dissolution profiles of the spray-dried nanoparticle agglomerates were also  
108 assessed. A full factorial design and standard least squares model were employed  
109 to understand the critical formulation parameters as well as any interactions  
110 between them involved in the wet milling and spray drying process and finally in  
111 the formation of respirable nanoparticle agglomerates. The critical formulation  
112 parameters investigated were: type of stabilizer, mannitol to drug ratio and leucine  
113 to drug ratio. The yield of the process, the particle size distribution, the  
114 redispersibility and the fine particle fraction were investigated as responses. To  
115 the best of our knowledge, it is the first time that such a study is carried out  
116 focusing on respirable nanoparticle agglomerates of a low melting drug.  
117

118 **2. Materials and methods**

119

120 **2.1. Materials**

121 Ibuprofen (IBU, Shasun Pharmaceuticals, India) with volume mean diameter  $D_{4,3}$ :  
122  $64.5 \pm 8.3 \mu\text{m}$  was used. Pharmacoat 603 (low viscosity hypromellose, HMPC  
123 2910, Shin-Etsu Chemical Co., Japan) and D- $\alpha$ -tocopherol polyethylene glycol  
124 1000 succinate (TPGS, Sigma Aldrich, USA) were used as stabilizers. Mannitol  
125 (Pearlitol<sup>®</sup> 160C, Roquette Frères, Lestrem, France) and L-leucine (Sigma  
126 Aldrich, USA) were used as a matrix former and a dispersibility enhancer of the  
127 nanoparticle agglomerates, respectively. Hyclone<sup>™</sup> Water for Injections (Thermo  
128 Scientific, UK) was used for the preparation of nanosuspensions. Methanol and  
129 acetonitrile were HPLC grade and all other reagents were of analytical grade.

130

131 **2.2. Methods**

132 **2.2.1. Preparation of nanosuspensions**

133 Nanosuspensions were prepared by wet bead milling using a laboratory planetary  
134 mill (Pulverisette 5, Fritsch Co., Germany). 0.5 g IBU, the stabilizer (10% w/w of  
135 IBU) and 10 g of milling beads (0.5 mm diameter aluminium borosilicate glass  
136 grinding beads, Gerhardt, UK) were weighed into each glass vial of 14 mL  
137 capacity and suspended in 10 mL Water for Injections. The vials were placed into  
138 a stainless steel milling pot with a maximum loading capacity of 8 vials. Rotation  
139 speed (200 rpm), milling duration (6 cycles) and stabilizer concentration (10%  
140 w/w of IBU) were selected based on preliminary studies. Each milling cycle  
141 comprised 30 min rotation followed by 20 min pause. At each pause, the  
142 nanocrystal size was determined and at the end of the milling procedure, the  
143 nanosuspensions were allowed to cool to room temperature and collected by  
144 withdrawal using a pipette for separation from the milling beads.

145 **2.2.2. Particle size distribution of nanosuspensions**

146 Malvern Nano ZS (Malvern Instrument, UK) was used for size measurements by  
147 dynamic light scattering (DLS) yielding the intensity-weighted mean  
148 hydrodynamic diameter of the bulk population (z-average) and the polydispersity  
149 index (PI) as a measure of the width of size distribution. 20  $\mu\text{L}$  of nanosuspension  
150 was diluted with 10 mL of saturated IBU solution, prepared by filtration of a

151 suspension through a 0.1  $\mu\text{m}$  disposable syringe filter to avoid extensive  
152 dissolution and was then shaken vigorously for 30 s by hand before being  
153 transferred to disposable sizing cuvettes. The measuring parameters were:  
154 dispersant refractive index of 1.338 and viscosity of dispersion medium 0.89 cP.  
155 All measurements were performed in triplicate.

### 156 **2.2.3. Preparation of nanoparticle agglomerates**

157 The obtained nanosuspensions were solidified by spray drying immediately after  
158 preparation. 10 mL of nanosuspension were diluted to 100 mL with an aqueous  
159 solution of mannitol and/or leucine to obtain the proportions reported in Table 1.  
160 Spray drying was performed using a laboratory scale spray dryer (Mini B-290,  
161 Buchi Labortechnik, Switzerland) fitted with a high performance cyclone. On the  
162 basis of preliminary experiments, the following parameters were employed: inlet  
163 temperature of 70  $^{\circ}\text{C}$ , outlet temperature of  $50 \pm 2^{\circ}\text{C}$ , feed rate of 5  $\text{mL min}^{-1}$  and  
164 atomizing gas flow rate of 0.5  $\text{L s}^{-1}$ . The collected nanoparticle agglomerates were  
165 weighed and stored in a desiccator over silica gel for subsequent testing.

### 166 **2.2.4. Determination of yield**

167 Yield was calculated as the ratio of the mass of the particles collected after spray  
168 drying to the mass of solids (drug and excipients) introduced in the feed suspension.  
169 The drug quantity used in the calculations was the amount weighed in the milling  
170 pots before the wet-milling step.

171

### 172 **2.2.5. Characterization of nanoparticle agglomerates**

#### 173 **2.2.5.1. Particle size analysis**

174 Particle size distributions of the nanoparticle agglomerates were determined by  
175 laser diffraction using a HELOS/ BR laser diffractometer (Sympatec, Germany)  
176 which was fitted with the micro-dosing unit ASPIROS and the dry disperser  
177 RODOS. Samples were placed in the feeder and pressurized air at 4 bar was used  
178 to disperse them in the measurement chamber, while the feeding velocity was kept  
179 constant at 50  $\text{mm s}^{-1}$ . An R2 lens detector (0.25- 87.5  $\mu\text{m}$ ) and the particle size  
180 distribution analysis software Windox 5 (Sympatec, Germany) were used. The  
181  $D_{10}$ ,  $D_{50}$  and  $D_{90}$  particle sizes (i.e. the size in microns at which 10%, 50% and



182 90% of the particles are smaller) were recorded. Measurements were carried out  
183 in triplicate.

184

#### 185 **2.2.5.2. Scanning electron microscopy**

186 The morphology of the starting materials and the nanoparticle agglomerates was  
187 investigated using scanning electron microscopy (SEM). Samples were placed on  
188 to double-sided electro-conductive adhesive tape, which was fixed onto an  
189 aluminium stub and then sputter-coated with gold (10 nm thickness). SEM  
190 micrographs were taken using a FEI Quanta 200 FEG ESEM (FEI, Netherlands),  
191 at 5.00 kV.

192

#### 193 **2.2.5.3. X-ray powder diffraction**

194 X-ray powder diffraction (XRPD) was employed to assess the crystallinity of the  
195 starting materials and the nanoparticle agglomerates. XRPD patterns were  
196 obtained with a bench-top diffractometer (Rigaku Miniflex 600, Japan). Cu K $\alpha$   
197 radiation at 15 mA and 40 kV with a step of 0.02 deg and a speed of 5 deg min<sup>-1</sup>  
198 was used, covering a 2  $\theta$  of 5-40 °. Miniflex Guidance (Rigaku, Japan) was the  
199 analysis software.

#### 200 **2.2.5.4. Differential scanning calorimetry**

201 Differential scanning calorimetry (DSC) was performed using a TA DSC Q200  
202 calorimeter (TA Instruments, USA) previously calibrated with indium. Accurately  
203 weighed powder samples (1-3 mg) were sealed into crimped standard aluminium  
204 pans (TA) and heated under nitrogen flow (50 mL min<sup>-1</sup>) from 25 °C to 30 °C  
205 above the expected melting point at a heating rate of 10 °C min<sup>-1</sup>.

#### 206 **2.2.5.5. Thermogravimetric analysis**

207 Thermogravimetric analysis (TGA) was used for determining the residual  
208 moisture content of the spray-dried formulations. TGA was performed with a  
209 Discovery TGA (TA Instruments, USA) controlled by TRIOS (TA) software.  
210 Weighted powder samples (1-5 mg) were placed into aluminium cups (TA) and  
211 heated under nitrogen flow (50 mL min<sup>-1</sup>) from 25 to 120 °C at a heating rate of  
212 10 °C min<sup>-1</sup>. The residual moisture content was calculated as the weight loss  
213 between 25 and 120 °C.

214 **2.2.5.6. Drug loading**

215 5 mg of nanoparticle agglomerates were dissolved in 50 mL methanol, and  
216 ibuprofen concentration was assayed using an HPLC system (Agilent 1100 Series,  
217 Agilent technologies, Germany). The stationary phase was a Luna® (150 x 4.60  
218 mm, 5 micron) column (Phenomenex Co., California, USA) kept at 30 °C. The  
219 mobile phase comprised acetonitrile and aqueous trifluoroacetic acid solution  
220 (0.1% v/v) at 50/50 volumetric ratio. The mobile phase flow rate was 1 mL min<sup>-1</sup>,  
221 the injection volume was 10 µL and the detection wavelength 214 nm. The  
222 retention time for ibuprofen was 7.4 min. The correlation coefficient of the  
223 calibration curve was R<sup>2</sup>=0.9999 for a concentration range of 5-600 µg mL<sup>-1</sup>,  
224 indicating acceptable linearity.

225 **2.2.5.6. Redispersibility**

226 Redispersibility index (RDI%) was determined according to Yue et al. [13]:

227 
$$RDI\% = \frac{z - average}{z - average_0} * 100.$$

228 where, *z-average*<sub>0</sub> is the intensity-weighted mean particle diameter of the  
229 nanosuspensions prior to spray drying measured by DLS and *z-average* is the  
230 corresponding value of nanosuspension reconstituted from nanoparticle  
231 agglomerates upon rehydration. For the measurement of redispersibility, around  
232 100 mg of each spray-dried powder was added to a glass vial containing 10 mL of  
233 an aqueous saturated IBU solution and it was shaken vigorously for 30s by hand  
234 before being transferred to disposable sizing cuvettes. The saturated solution of  
235 ibuprofen was prepared by filtration of a drug suspension through a 0.1 µm  
236 disposable syringe filter in order to avoid extensive dissolution. A RDI value close  
237 to 100% indicates that the spray-dried nanoparticle agglomerates exhibit complete  
238 reconstitution after rehydration to particles of similar size as the primary  
239 nanocrystals after nanomilling and before the solidification step.

240 **2.2.5.7. In-vitro dissolution testing**

241 The paddle method was applied by using USP apparatus type II (Pharma Test,  
242 Germany), at 37 °C and 50 rpm stirring speed. The dissolution medium was 500  
243 mL of deionised water (freshly boiled and cooled, pH: 6-7). At specific time

244 intervals up to 120 min, 5 mL of dissolution medium was withdrawn, filtered  
245 through a 0.1  $\mu\text{m}$  disposable syringe filter and placed in HPLC vials for assay,  
246 whilst being immediately replaced with 5 mL of fresh medium. The HPLC  
247 conditions for the assay were as for drug content determination. Dissolution tests  
248 were conducted in triplicate for each formulation.

249

#### 250 **2.2.5.8. *In-vitro* aerosol performance**

251 The aerodynamic assessment of the nanoparticle agglomerates was carried out  
252 using the fast screening impactor, FSI (MSP 185 FSI, Copley Scientific, UK). The  
253 FSI was developed based on the abbreviated impactor measurement concept. It  
254 divides the particles discharged from the inhaler into two parts: the coarse fraction  
255 and the fine fraction (aerodynamic diameter less than 5  $\mu\text{m}$ ). The coarse fraction  
256 collector was equipped with an insert that enables a cut-off of 5  $\mu\text{m}$  at 30 L  $\text{min}^{-1}$ .  
257 The particles not captured in the coarse fine collector followed the airstream and  
258 deposited in the fine fraction collector where a filter captured all of them. The FSI  
259 was connected to a high-capacity vacuum pump (Model HCP5, Copley  
260 Instruments, UK). Based on results from preliminary studies the bottom plate of  
261 the pre-separator was coated with 1% w/v silicone oil in hexane in order to reduce  
262 particle bounce that is created from the additional 5  $\mu\text{m}$  cut-off plate. The actual  
263 flow rate was measured using a calibrated flow meter (Flow Meter Model DFM  
264 2000, Copley Instrument Ltd, UK) prior to each run, to ensure that a flow at 30 L  
265  $\text{min}^{-1}$  was achieved. Gelatin hard capsules (size 3) were filled with accurately  
266 weighed amounts of product (ranging from 12.5 to 28 mg depending on the drug  
267 loading of each formulation) corresponding to about 10 mg of IBU. The capsules  
268 were placed in the inhaler device (Cyclohaler®) fitted to the impactor via an  
269 airtight rubber adaptor and tested at 30 L  $\text{min}^{-1}$  for 8 s (total volume: 4 L). The  
270 capsules were discharged into the FSI and after dispersion the particles were  
271 collected on a glass fiber filter (76 mm, Pall Corporation, USA) and extracted in  
272 methanol. Analysis of the extracts from the capsules, mouthpiece and each part of  
273 the FSI was performed with HPLC. The HPLC conditions for the assay were as  
274 for drug content determination. Each formulation was tested in triplicate. The fine  
275 particle fraction (FPF%) of the formulations was the ratio of the drug mass  
276 depositing on the fine fraction collector divided by the recovered dose. The fine

277 particle dose (FPD) was calculated as the total mass deposited on the fine fraction  
278 collector divided by the number of doses (n=3).

279

#### 280 **2.2.5.9. Design of Experiments**

281 A full factorial design  $2^3$  (3 factors at 2 levels) was used allowing the estimation  
282 of the main effects and the two-way interactions. The three independent variables  
283 used at two levels in the design were: type of stabilizer ( $X_1$ ), mannitol to drug ratio  
284 ( $X_2$ ) and leucine to drug ratio ( $X_3$ ). Dependent variables: yield, volume median  
285 diameter ( $D_{50}$ ), redispersibility index (RDI%) and fine particle fraction (FPF%),  
286 were selected as responses (Table 1). The design matrix included 8 runs plus four  
287 centre points (Fig. 1). Centre points were added to the design space to identify any  
288 non-linearity in the responses. The design space was constructed and analyzed  
289 using the JMP 12.1.0 software (SAS Institute, USA). To reduce systematic errors,  
290 all the experiments were completely randomized. The standard least squares model  
291 (including multiple linear regression analysis and ANOVA) was fitted in to model  
292 the data. The significance and validity of the model was estimated by ANOVA.  
293 The parameter estimates and the probability values (p-values) of the effects and  
294 two-way interactions of each response are given. p-values less than 0.05 were  
295 deemed to be statistically significant.

296

297 **3. Results and discussion**

298 **3.1. Preparation and characterization of nanosuspensions**

299 Both stabilizers were able to produce nanosuspensions of ibuprofen after 180 min  
300 of wet milling. The results of z-average size and polydispersity index (PI) of  
301 nanosuspensions obtained with both stabilizers as a function of milling time are  
302 presented in (Fig. 2). More specifically, after 180 min nanosuspensions stabilized  
303 with HPMC and TPGS exhibited a z-average size of  $533 \pm 28$  nm and  $663 \pm 12$   
304 nm, respectively.

305

306 The starting material, with a volume mean diameter  $D_{4,3}$ :  $64.5 \pm 8.3$   $\mu\text{m}$  (Fig. 3)  
307 initially showed rapid size reduction during milling, especially with HPMC as  
308 stabilizer. In the case of HPMC, submicron particles of ibuprofen were produced  
309 in 60 min while for TPGS this occurred in 90 min. The breakage rate of crystals  
310 was high initially and with further milling time the size continued to decrease, but  
311 at a slower rate for both stabilizers. This is a common profile as breakage rate  
312 kinetics have been found to follow a first-order exponential decay [35].

313

314 In the study of Nihei et al. [27], thymoquinone, a low melting compound (m.p. 46  
315 °C) with antioxidant properties had to be nanosized using a cold wet-milling  
316 system in order to avoid the formation of large aggregates that were caused by the  
317 partial melting of the compound when a wet mill without a heat exchanger was  
318 used. In this study, no aggregation of ibuprofen was observed during milling  
319 indicating that cautious selection of the process parameters (i.e. a lower milling  
320 speed and an increased milling time with intervals so as to cool down the vessels)  
321 could allow the use of wet mills which are not equipped with temperature control  
322 accessories for the nano-comminution of low melting drugs. This could be  
323 especially applicable to preformulation research at preclinical and clinical studies  
324 where limited resources are available (i.e. time, equipment, investment, compound).

325

326 The results reported in this study can be favorably compared with those obtained  
327 by rapid expansion of supercritical solutions [36] and high pressure  
328 homogenization [37], as both methods could not produce ibuprofen crystals with  
329 size in the submicrometre scale.

330

331 Comminution of ibuprofen in water using a Lena DM 100 nanoparticle production  
332 machine, equipped with a heat exchanger and operating in the recirculation mode,  
333 resulted in nanosuspensions with z-average size around 450 nm [38]. The smaller  
334 size of nanocrystals reported may be attributed to the use of a combination of  
335 polymers and surfactants as stabilizers, and this also indicates the scalability of  
336 wet milling in industrial settings [39].

337

### 338 **3.2. Yield**

339 The yield was selected as a response characterizing quantitatively the overall  
340 productivity of the process. For the experimental conditions applied the yield  
341 ranged from 27.3% to 72.5% (Table 1). The generated model was significant and  
342 the response was modeled with high accuracy (adjusted  $R^2$ : 0.96, Table 2).

343

344 All the three independent variables were identified as significant with a positive  
345 effect on the yield of the process ( $p < 0.05$ , Table 2). The positive effect of  
346 increasing the leucine and mannitol to drug ratios may be attributed to the  
347 increased concentration of the solids dissolved in the feed suspension, prior to the  
348 spray-drying step. Spray drying of nanosuspensions stabilized with TPGS led to  
349 the lowest yield of 27.3%. This low yield may be attributed to the low melting  
350 point of TPGS resulting in melting and adhesion of the nanoparticle agglomerates  
351 to the drying chamber and cyclone. Replacing TPGS with HPMC, which is a non-  
352 thermolabile stabilizer increased the yield. The yield of the process was found to  
353 maximize by increasing the leucine to drug ratio. This may be explained by the  
354 fact that leucine accumulates on the surface of the particles forming a coating  
355 around them and thus protecting them from high temperatures during spray drying.  
356 Similar results were reported regarding the spray drying of hydro-alcoholic  
357 solutions of  $\beta$ -estradiol where the powder yield increased with increasing leucine  
358 content in the formulation [40]. The explanation proposed by the authors was that  
359 when increasing leucine content was used, the drug was encapsulated in micelle-  
360 like structures of leucine and thus was protected from the relative harsh spray-  
361 drying conditions.

362 As shown in the surface plots (Fig. 6a,b) higher yields are obtained when HPMC  
363 was used as the stabilizer of ibuprofen nanosuspensions, and when high leucine

364 and mannitol to drug ratios were used in the formulations prior to the spray-drying  
365 step.

366

### 367 **3.3. Characterization of nanoparticle agglomerates**

#### 368 **3.3.1. Particle size and morphology**

369 The SEM images of the formulations prepared based on the full factorial design  
370 are shown in Fig. 4,5. Spray drying of ibuprofen nanosuspensions stabilized either  
371 by HPMC or TPGS in the absence of excipients resulted in aggregated particles of  
372 irregular morphology with size outside the acceptable range for pulmonary drug  
373 delivery (Table 1 and Fig.4,5).

374

375 Addition of mannitol and/or leucine resulted in the promotion of spherical particles  
376 with mean size approximately 2-3  $\mu\text{m}$  that is suitable for pulmonary drug delivery.  
377 The surface of the spray-dried particles appears not to be smooth and a closer  
378 inspection reveals the presence of nanoparticles indicating the composite structure  
379 of the particles where ibuprofen nanocrystals are embedded in a matrix of mannitol  
380 and/or leucine (i.e. nanoparticle agglomerates).

381

382 The nanoparticle agglomerates containing leucine consist of individual particles  
383 (e.g. patterns 1-+, 2-+, Fig.4,5). This may be attributed to the accumulation of  
384 leucine at the surface of the particles preventing any particle fusion. A high leucine  
385 to drug ratio resulted in wrinkled particles (patterns 1++, 2++, Fig.4,5). A wrinkled  
386 morphology was interpreted as an indication of hollow particles as the particle  
387 density was found to decrease as the “wrinkleness” of the particles was increased  
388 [41].

389

390 The nanoparticle agglomerates appear to be porous with holes and dimples in the  
391 particle surface due to the evaporation of liquid that escapes from the inner of the  
392 droplet through the solid crust built up in the course of the drying process on the  
393 surface of the droplet [15,42]. Engineering of porous particles is considered  
394 beneficial for pulmonary drug delivery as particles with high porosity have smaller  
395 aerodynamic diameter compared to non-porous particles of the same physical size,  
396 increasing the probability for deposition in the lower respiratory tract [43].

397

398 The particle size of the nanoparticle agglomerates obtained was measured by laser  
399 diffraction as a volume diameter (Table 1). The dried powders obtained exhibited  
400 a median diameter  $D_{50}$  between 2.15 and 16.04  $\mu\text{m}$  and the data are in good  
401 agreement with the particle size observed by SEM. The results were analyzed in  
402 the experimental design performing ANOVA for particle size, focusing on the  $D_{50}$   
403 value and the model was found significant ( $p < 0.05$ , Table 2).

404

405 Leucine to drug ratio and the type of stabilizer used were identified as formulation  
406 variables with the most significant effects on the  $D_{50}$  (Table 2). Their “negative”  
407 effect is interpreted as size reduction, which is desirable for pulmonary drug  
408 delivery. The observation regarding the influence of leucine on particle size is in  
409 agreement with the study of Sou et al. [20] in which it was reported that leucine in  
410 contrast to glycine and alanine was the only amino acid that reduced the  $D_{50}$  when  
411 added into the mannitol formulations. Also, it is likely that increased leucine to  
412 drug ratio enhanced surface coating around the particles, which prevented the  
413 particles from melting and sintering, as observed for the process yield.

414

415 A significant interaction was identified between leucine to drug ratio and the type  
416 of stabilizer, with a positive parameter estimate, despite the fact that the factors  
417 had individually negative effects on the  $D_{50}$  (Table 2), indicating a synergistic  
418 rather than an additive interaction between HPMC and leucine to drug ratio. Use  
419 of the non-melting HPMC as a nanosuspension stabilizer and the addition of a high  
420 leucine to drug ratio leads to further particle size reduction than the individual  
421 factors alone.

422 As shown in the surface plot, spray drying of ibuprofen nanosuspensions stabilized  
423 with HPMC and containing a high leucine to drug ratio is able to produce  
424 nanoparticle agglomerates with particle size around 2-3  $\mu\text{m}$  that is suitable for  
425 pulmonary drug delivery (Fig. 6c). On the other hand, spray drying of ibuprofen  
426 nanosuspensions stabilized with TPGS results in larger particles, while addition of  
427 both high leucine and mannitol to drug ratios was required in order to produce  
428 particles smaller than 4  $\mu\text{m}$  (Fig. 6d). This indicates that the selection of stabilizer  
429 is vital not only for the step of nanosuspension production, but it may also



430 influence the downstream process of spray drying by affecting the properties of  
431 the nanoparticle agglomerates produced.

### 432 **3.3.2. Redispersibility**

433 Redispersibility is an important quality attribute of nanoparticle agglomerates as  
434 it is a prerequisite for the reformation of nanoparticles upon rehydration of the  
435 larger particles with potential enhancement of therapeutic efficacy. Particularly,  
436 for nanoparticles of low melting drugs such as ibuprofen, thermal stresses during  
437 spray drying may lead to phase and composition changes of formulations causing  
438 irreversible aggregation and loss of the advantages of nanoformulations [12]. An  
439 RDI% value close to 100% means that the nanoparticle agglomerates reformed  
440 nanoparticles with z-average size close to the z-average size of the primary  
441 nanoparticles prior to the solidification step. For the experimental conditions  
442 applied, the redispersibility index (RDI%) ranged from 148 % to 938% (Table 1).  
443 The redispersibility results were analyzed in the experimental design performing  
444 ANOVA for particle size focusing on the RDI% value and the model was found  
445 significant ( $p < 0.05$ , Table 2).

446

447 The mannitol to drug ratio was identified as the only significant factor affecting  
448 redispersibility ( $p < 0.05$ , Table 2) with higher mannitol to drug ratio leading to  
449 RDI% values closer to 100%. The role of mannitol as a redispersibility enhancer  
450 can be explained by the formation of a continuous matrix around the nanocrystals  
451 during the spray-drying step, preventing their irreversible aggregation. Upon  
452 rehydration, mannitol as a hydrophilic excipient dissolves and the  
453 nanosuspensions are reconstituted.

454

455 As shown in the surface plots (Fig. 7a,b), nanoparticle agglomerates of ibuprofen  
456 with enhanced redispersibility (RDI% value close to 100%) were obtained only  
457 when high mannitol to drug ratios are present in the formulations prior to the spray-  
458 drying step.

### 459 **3.3.3. Drug loading**

460 The results of assayed ibuprofen content in the nanoparticle agglomerates are  
461 given in Table 3. Spray drying of nanosuspensions without mannitol and/or leucine  
462 appeared to have lower drug loading than the nominal. This may be attributed to

463 the melting of TPGS during spray drying that led to drug loss due to deposition on  
464 the walls of the drying chamber and cyclone. For the spray-dried nanosuspensions  
465 containing mannitol and/or L-leucine the assayed ibuprofen content is close to the  
466 nominal content indicating that the addition of these excipients prevented  
467 ibuprofen loss or powder segregation during the production process.

468

#### 469 **3.3.4. Solid state characterization**

470 The XRPD patterns of the starting materials are shown in Fig.8a. Raw ibuprofen  
471 exhibited sharp peaks in the range of 2 theta: 15-25 ° that are characteristic of the  
472 drug [38,44]. Mannitol starting material exhibited characteristic peaks of the β-  
473 form (2 theta: 10.6°, 14.7°, 16.9°, 21.2°, 23.9°, 29.5°) [45] while the diffractogram  
474 of L-leucine indicated a highly crystalline structure (2 theta: 6°, 12°, 24°, 31°, 37°)  
475 [46].

476

477 The diffractograms of all runs prepared according to the DoE are shown in Fig.  
478 8b. The diffractograms of patterns 1-- and 2-- (without matrix former and  
479 dispersibility enhancer) showed peaks at similar 2 theta positions to those of the  
480 raw ibuprofen. For the nanoparticle agglomerates of ibuprofen containing  
481 mannitol and/or leucine, the diffractograms were a summation of the patterns of  
482 their components. No new peaks or halo could be detected in the XRPD patterns  
483 indicating the absence of generated amorphous content during the process.

484

485 The DSC was used to assess the thermal behaviour of the starting materials and  
486 nanoparticle agglomerates of ibuprofen (Fig. 9). The DSC thermogram of  
487 ibuprofen showed an endothermic peak at 76 °C corresponding to the melting of  
488 the drug. The nanoparticle agglomerates of ibuprofen without mannitol and  
489 leucine exhibited the same endothermic peak shifted to a slightly lower  
490 temperature (Fig. 9a), while those containing mannitol exhibited thermal  
491 behaviour depending on the stabilizer.

492

493 More specifically, the nanoparticle agglomerates of ibuprofen containing mannitol  
494 and stabilized with TPGS exhibited two endothermic peaks (patterns 2++, 2+-,  
495 Fig. 9b) as expected: the melting peak at around 70 °C, which relates to the melting  
496 of the drug and a sharp endothermic peak at 168 °C which relates to the melting of

497 mannitol (Pearlitol: 160 °C). For the nanoparticle agglomerates of ibuprofen  
498 containing mannitol and stabilized with HPMC, apart from the melting of  
499 ibuprofen, an endothermic peak at 150 °C was followed by an exothermic event  
500 and then an endothermic melting at 168 °C (patterns 1++, 1+-, Fig. 9b). The  
501 thermal events observed in the DSC of patterns 1++ and 1+- could be attributed to  
502 the formation of the metastable  $\delta$ -form of mannitol (m.p. 150-158 °C) that is  
503 followed by crystallization to the  $\alpha$ - or/and  $\beta$ -form, and the melting of the  
504 respective crystal form [47]. Both  $\alpha$ - and  $\delta$ -form of mannitol were found to be  
505 chemically and physically stable for at least 5 years when stored at 25 °C and 43%  
506 relative humidity [47]. Recently, co-spray drying of an aqueous solution of  
507 mannitol with PVP in a ratio 4:1 was reported to produce the  $\delta$ -form of mannitol  
508 [48].

509

510 Overall, the XRPD and DSC data suggest that the engineered nanoparticle  
511 agglomerates retain their crystallinity during wet bead milling followed by spray  
512 drying. The preservation of the crystalline state is advantageous, ensuring the long-  
513 term physical stability of the formulations during storage.

514

### 515 **3.3.5. Residual moisture content**

516 Thermogravimetric analysis of the spray-dried powders indicated that the moisture  
517 content of the powders ranged from 1.1 to 4.7% w/w (Table 3). These values  
518 compare favourably with other studies which report moisture content of spray-  
519 dried powders in the region of 5-10% w/w [49,50]. Specifically, residual moisture  
520 content ranged from 2.3 to 4.7% for the nanoparticle agglomerates stabilized with  
521 HPMC and from 1.1 to 2.3% for those stabilized with TPGS and it was reduced  
522 for the agglomerates with high mannitol to drug ratio (Table 3). This is in  
523 agreement with the results reported by Yamasaki et al. [7], that increasing mannitol  
524 content in nanomatrix powders of ciclosporin A reduced the residual moisture  
525 content of the formulations, which was attributed to its non-hygroscopic nature.  
526 Thus, despite the low inlet (70 °C) and outlet temperature (50 °C), selected to  
527 prevent melting of the drug during spray drying, addition of mannitol can  
528 minimize the moisture content of the nanoparticle agglomerates that is required  
529 for quality reasons (e.g. physical and chemical stability, reduced cohesiveness  
530 during storage, non-aggregation) [51].

531 **3.3.6. *In-vitro* dissolution tests**

532 The dissolution profiles of ibuprofen and the nanoparticle agglomerates prepared  
533 according to the matrix of the full factorial design are shown in Fig. 10.  
534 Nanoparticle agglomerates stabilized with either HPMC or TPGS exhibited  
535 enhanced dissolution profiles compared to ibuprofen. In the case of the raw  
536 ibuprofen, less than 40% was released in the first 20 min, while the nanoparticle  
537 agglomerates achieved complete dissolution in less than 5 min. The exceptions to  
538 this were the spray-dried nanosuspensions of ibuprofen without matrix former  
539 (patterns 1-- and 2--) which exhibited a higher dissolution rate compared to  
540 ibuprofen but slower than the nanoparticle agglomerates containing mannitol  
541 and/or leucine. In the case of TPGS, this may be associated with the formation of  
542 large aggregates with size around 50  $\mu\text{m}$  and poor redispersibility (Fig. 5). Thus,  
543 the selection of suitable process and formulation parameters is of paramount  
544 importance in order to ensure that the dissolution benefit of nanoparticles is  
545 retained after spray drying.

546

547 **3.3.7. *In-vitro* aerosol performance**

548 Fine particle fraction (FPF) was selected as a quality attribute describing the  
549 aerodynamic performance of a dry powder for inhalation. The European  
550 Pharmacopoeia (2.9.18 preparations for inhalation: aerodynamic assessment of  
551 fine particles, Ph. Eur. 8.0) suggest that a pressure drop over the inhaler of 4 kPa  
552 is broadly representative of the pressure drop generated by the patients using dry  
553 powder inhalers during inhalation [52]. In this study, operating a ‘medium’  
554 resistance device as Cyclohaler® at 30 L min<sup>-1</sup> leads to a low pressure drop across  
555 the inhaler. While this low pressure drop across the inhaler reduces the probability  
556 of establishing comparable *in-vitro* performance and *in-vivo* drug deposition, it is  
557 considered acceptable for comparing the *in-vitro* aerosolisation performance of  
558 formulations prepared in this study. The FPF values of the nanoparticle  
559 agglomerates produced ranged from 5.84 to 68.55% (Table 1) and the model  
560 generated was found to be significant ( $p < 0.05$ , Table 2).

561

562 Leucine to drug ratio and mannitol to drug ratio were identified as the most  
563 significant factors on the FPF (Table 2.). The positive effect of leucine can be  
564 linked with its properties as a dispersibility and aerosolization enhancer. In

565 contrast to other amino acids such as alanine and glycine, leucine has been found  
566 to reduce capsule retention and increase both the emitted and the fine particle  
567 fraction of formulations [20,22]. For spray-dried particles of salbutamol sulfate  
568 and lactose containing increasing amount of leucine (5-20% w/w), Seville et al  
569 [22] observed an increase of the FPF% (from 50% to 80%, respectively). In  
570 another study, Sou et al. [20] reported the highly significant and positive effect of  
571 leucine on improving the FPF% of spray-dried mannitol particles.

572

573

574 Regarding the positive effect of mannitol to drug ratio, it may be attributed to the  
575 good spray-drying properties of mannitol which facilitates the formation of  
576 spherical particles with narrow and unimodal particle size distribution [15,53].

577

578 As illustrated in the surface plots (Fig. 7c, d), both leucine and mannitol to drug  
579 ratio have a significant effect on the aerodynamic performance of the nanoparticle  
580 agglomerates, resulting in a large FPF increase from 10% to over 65%. Therefore,  
581 a combination of high leucine and mannitol to drug ratios is required in order to  
582 maximise the FPF of the nanoparticle agglomerates of the low melting and ductile  
583 ibuprofen.

584

#### 585 **4. Conclusions**

586 Nanosuspensions of the poorly water-soluble, low melting point and ductile drug  
587 ibuprofen stabilized with HPMC and TPGS were successfully produced and were  
588 further spray dried with or without the addition of excipients (mannitol and/or L-  
589 leucine) employing a full factorial design. Design of experiments is a useful  
590 approach in order to gain insight into the formation of inhalable nanoparticle  
591 agglomerates using wet milling followed by spray drying. Leucine to drug ratio,  
592 mannitol to drug ratio and the type of stabilizer were found to be significant  
593 ( $p<0.05$ ) factors affecting the yield of the particles obtained by combining wet  
594 milling and spray drying. The particle size response was mainly dependent on the  
595 leucine to drug ratio and the type of stabilizer employed ( $p<0.05$ ). Mannitol to  
596 drug ratio was found to be the only critical parameter affecting redispersibility of  
597 nanoparticle agglomerates ( $p<0.05$ ), and both leucine to drug ratio and mannitol  
598 to drug ratio were found to be significant factors affecting FPF ( $p<0.05$ ). While

599 the importance of the type of stabilizer on the formation of nanosuspensions has  
600 been previously reported [33,54,55], in this study it was observed that the selection  
601 of stabilizer could also influence the downstream process of spray drying by  
602 affecting the yield and the particle size distribution of the resultant nanoparticle  
603 agglomerates. Moreover, the nanoparticle agglomerates were found to be  
604 crystalline which is advantageous for their physical stability upon storage, and they  
605 exhibit enhanced dissolution compared to the ibuprofen starting material. Overall,  
606 it appears that by selecting the stabilizer and adjusting the mannitol and leucine to  
607 drug ratio during the spray drying of nanosuspensions can result in nanoparticle  
608 agglomerates with enhanced dissolution and aerosolization behaviour despite the  
609 challenging properties (thermal and mechanical) of a drug as ibuprofen.

#### 610 **Acknowledgements**

611 EPSRC Centre of Doctoral Training in Targeted Therapeutics and Formulation  
612 Sciences for the funding of this project (EP/I01375X/1). Mr David McCarthy  
613 (UCL) is thanked for taking the SEM images.

614

## References

- [1] J. Chingunpituk, Nanosuspension technology for drug delivery, *Walailak J. Sci. Tech.* 4 (2007) 139–153.
- [2] J.M. Butler, J.B. Dressman, The developability classification system: application of biopharmaceutics concepts to formulation development, *J. Pharm. Sci.* 99 (2010) 4940–4954.
- [3] J.P. Möschwitzer, Drug nanocrystals in the commercial pharmaceutical development process, *Int. J. Pharm.* 453 (2013) 142–156.
- [4] B. Van Eerdenbrugh, G. Van den Mooter, P. Augustijns, Top-down production of drug nanocrystals: nanosuspension stabilization, miniaturization and transformation into solid products, *Int. J. Pharm.* 364 (2008) 64–75.
- [5] M. Malamatari, S. Somavarapu, K.M.G. Taylor, G. Buckton, Solidification of nanosuspensions for the production of solid oral dosage forms and inhalable dry powders, *Expert Opin. Drug Deliv.* 13 (2016) 435–450.
- [6] A.S. Mujumdar, D.S. Alterman, Drying in the pharmaceutical and biotechnology fields, in: E. Goldberg (Ed.), *Handbook of Downstream Processing*, Springer Netherlands, Dordrecht, 1997: pp. 235–260.
- [7] K. Yamasaki, P.C.L. Kwok, K. Fukushige, R.K. Prud'homme, H.-K. Chan, Enhanced dissolution of inhalable cyclosporine nano-matrix particles with mannitol as matrix former, *Int. J. Pharm.* 420 (2011) 34–42.
- [8] C. Duret, N. Wauthoz, T. Sebti, F. Vanderbist, K. Amighi, New inhalation-optimized itraconazole nanoparticle-based dry powders for the treatment of invasive pulmonary aspergillosis, *Int. J. Nanomedicine.* 7 (2012) 5475–5489.
- [9] A. Pomázi, F. Buttini, R. Ambrus, P. Colombo, P. Szabó-Révész, Effect of polymers for aerolization properties of mannitol-based microcomposites containing meloxicam, *Eur. Polym. J.* 49 (2013) 2518–2527.
- [10] M. Malamatari, S. Somavarapu, M. Bloxham, G. Buckton, Nanoparticle agglomerates of indomethacin: The role of poloxamers and matrix former on their dissolution and aerosolisation efficiency, *Int. J. Pharm.* 495 (2015) 516–526.
- [11] A.H. Chow, H.H. Tong, P. Chattopadhyay, B.Y. Shekunov, Particle engineering for pulmonary drug delivery, *Pharm. Res.* 24 (2007) 411–437.
- [12] M. V. Chaubal, C. Popescu, Conversion of nanosuspensions into dry powders by spray drying: a case study, *Pharm. Res.* 25 (2008) 2302–2308.
- [13] P.F. Yue, Y. Li, J. Wan, M. Yang, W.F. Zhu, C.H. Wang, Study on formability of solid nanosuspensions during nanodispersion and solidification: I. Novel role of stabilizer/drug property, *Int. J. Pharm.* 454 (2013) 269–277.
- [14] G. Pilcer, K. Amighi, Formulation strategy and use of excipients in pulmonary drug delivery, *Int. J. Pharm.* 392 (2010) 1–19.

- [15] S.G. Maas, G. Schaldach, E.M. Littringer, A. Mescher, U.J. Griesser, D.E. Braun, P.E. Walzel, N. A. Urbanetz, The impact of spray drying outlet temperature on the particle morphology of mannitol, *Powder Technol.* 213 (2011) 27–35.
- [16] R. Rowe, P. Sheskey, W. Cook, M. Fenton, *Handbook of Pharmaceutical Excipients*, 7th ed., Pharmaceutical Press, London, 2012.
- [17] B. Zuo, Y. Sun, H. Li, X. Liu, Y. Zhai, J. Sun, Z. He, Preparation and in vitro/in vivo evaluation of fenofibrate nanocrystals, *Int. J. Pharm.* 455 (2013) 267–75.
- [18] B. Van Eerdenbrugh, L. Froyen, J. Van Humbeeck, J. A. Martens, P. Augustijns, G. Van Den Mooter, Alternative matrix formers for nanosuspension solidification: Dissolution performance and X-ray microanalysis as an evaluation tool for powder dispersion, *Eur. J. Pharm. Sci.* 35 (2008) 344–353.
- [19] S. Kumar, R. Gokhale, D.J. Burgess, Sugars as bulking agents to prevent nano-crystal aggregation during spray or freeze-drying, *Int. J. Pharm.* 471 (2014) 303–311.
- [20] T. Sou, L. Orlando, M.P. McIntosh, L.M. Kaminskas, D.A.V. Morton, Investigating the interactions of amino acid components on a mannitol-based spray-dried powder formulation for pulmonary delivery: A design of experiment approach, *Int. J. Pharm.* 421 (2011) 220–229.
- [21] T. Sou, L.M. Kaminskas, T.H. Nguyen, R. Carlberg, M.P. McIntosh, D.A.V. Morton, The effect of amino acid excipients on morphology and solid-state properties of multi-component spray-dried formulations for pulmonary delivery of biomacromolecules, *Eur. J. Pharm. Biopharm.* 83 (2013) 234–243.
- [22] P. Seville, T.P. Learoyd, H.Y. Li, I.J. Williamson, J.C. Birchall, Amino acid-modified spray-dried powders with enhanced aerosolisation properties for pulmonary drug delivery, *Powder Technol.* 178 (2007) 40–50.
- [23] S. Mangal, F. Meiser, G. Tan, T. Gengenbach, J. Denman, M.R. Rowles, I. Larson, D.A. V Morton, Relationship between surface concentration of l-leucine and bulk powder properties in spray dried formulations, *Eur. J. Pharm. Biopharm.* 94 (2015) 160–169.
- [24] H. Leuenberger, The compressibility and compactibility of powder systems, *Int. J. Pharm.* 12 (1982) 41–55.
- [25] I. Larsson, H. Kristensen, Comminution of a brittle/ductile material in a Micros Ring Mill, *Powder Technol.* 107 (2000) 175–178.
- [26] K. Yuminoki, M. Takeda, K. Kitamura, S. Numata, K. Kimura, T. Takatsuka, N. Hashimoto, Nano-pulverization of poorly water soluble compounds with low melting points by a rotation/revolution pulverizer, *Pharmazie.* 67 (2012) 681–686.
- [27] T. Nihei, H. Suzuki, A. Aoki, K. Yuminoki, N. Hashimoto, H. Sato, Y. Seto, S. Onoue, Development of a novel nanoparticle formulation of thymoquinone with a cold wet-milling system and its pharmacokinetic analysis, *Int. J. Pharm.* 511 (2016) 455–461.
- [28] S. Onoue, N. Terasawa, T. Nakamura, K. Yuminoki, N. Hashimoto, S. Yamada, Biopharmaceutical characterization of nanocrystalline solid dispersion of coenzyme Q10



prepared with cold wet-milling system, *Eur. J. Pharm. Sci.* 53 (2014) 118–125.

- [29] M.L.A.D. Lestari, R.H. Müller, J.P. Möschwitzer, Systematic Screening of Different Surface Modifiers for the Production of Physically Stable Nanosuspensions, *J. Pharm. Sci.* 104 (2015) 1128–1140.
- [30] P. Shah, K. Marshall-Batty, M. Panzer, J. Smolen, J. Tagaer, C. Rodesney, H. Le, D. Gordon, W. Greenberg, C. Youngs, C. Lannon, Antimicrobial and synergistic effects of ibuprofen against resistant cystic fibrosis pathogens, in: 115th General Meeting of the American Society of Microbiology, 2015.
- [31] A.K. Yazdi, H.D.C. Smyth, Carrier-free high-dose dry powder inhaler formulation of ibuprofen: Physicochemical characterization and in vitro aerodynamic performance, *Int. J. Pharm.* 511 (2016) 403–414.
- [32] S. Verma, R. Gokhale, D.J. Burgess, A comparative study of top-down and bottom-up approaches for the preparation of micro/nanosuspensions, *Int. J. Pharm.* 380 (2009) 216–222.
- [33] B. Van Eerdenbrugh, J. Vermant, J.A. Martens, L. Froyen, J. Van Humbeeck, P. Augustijns, G. Van den Mooter, A screening study of surface stabilization during the production of drug nanocrystals, *J. Pharm. Sci.* 98 (2009) 2091–2103.
- [34] G. Perfetti, T. Alphazan, W.J. Wildeboer, G.M.H. Meesters, Thermo-physical characterization of Pharmacoat® 603, Pharmacoat® 615 and Mowiol® 4-98, *J. Therm. Anal. Calorim.* 109 (2012) 203–215.
- [35] A. Afolabi, O. Akinlabi, E. Bilgili, Impact of process parameters on the breakage kinetics of poorly water-soluble drugs during wet stirred media milling: A microhydrodynamic view, *Eur. J. Pharm. Sci.* 51 (2014) 75–86.
- [36] F. Cristini, M. Delalonde, C. Joussot-Dubien, B. Bataille, Elaboration of ibuprofen microcomposites in supercritical CO<sub>2</sub>, in: 6th International Symposium of Supercritical Fluids, 2003.
- [37] R. Mauludin, J. Moschwitzer, R. Müller, Fast dissolving ibuprofen nanocrystal-loaded solid dosage forms, *Int. J. Pharm. Pharm. Sci.* 4 (2012) 543–549.
- [38] S. Plakkot, M. de Matas, P. York, M. Saunders, B. Sulaiman, Comminution of ibuprofen to produce nano-particles for rapid dissolution, *Int. J. Pharm.* 415 (2011) 307–314.
- [39] E. Bilgili, M. Li, A. Afolabi, Is the combination of cellulosic polymers and anionic surfactants a good strategy for ensuring physical stability of BCS Class II drug nanosuspensions?, *Pharm. Dev. Technol.* (2015) 1–12.
- [40] N. Rabbani, P. Seville, The influence of formulation components on the aerosolisation properties of the spray-dried powders, *J. Control. Release.* 10 (2005) 130–140.
- [41] J. Raula, F. Thielmann, M. Naderi, V.P. Lehto, E.I. Kauppinen, Investigations on particle surface characteristics vs. dispersion behaviour of l-leucine coated carrier-free inhalable powders, *Int. J. Pharm.* 385 (2010) 79–85.

- [42] R. Vehring, Pharmaceutical particle engineering via spray drying, *Pharm. Res.* 25 (2008) 999–1022.
- [43] D.A. Edwards, J. Hanes, G. Caponetti, J. Hrkach, A. BenJebria, M. Lou Eskew, J. Mintzes, D. Deaver, N. Lotan, R. Langer, Large Porous Particles for Pulmonary Drug Delivery, *Science* 276 (1997) 1868–1871.
- [44] D. Kayrak, U. Akman, Ö. Hortaçsu, Micronization of Ibuprofen by RESS, *J. Supercrit. Fluids.* 26 (2003) 17–31.
- [45] W.L. Hulse, R.T. Forbes, M.C. Bonner, M. Getrost, The characterization and comparison of spray-dried mannitol samples, *Drug Dev. Ind. Pharm.* 35 (2009) 712–718.
- [46] J. Raula, A. Kuivanen, A. Lahde, H. Jiang, M. Antopolsky, J. Kansikas, E.I. Kauppinen, Synthesis of L-leucine nanoparticles via physical vapor deposition at varying saturation conditions, *J. Aerosol Sci.* 38 (2007) 1172–1184.
- [47] A. Burger, J.O. Henck, S. Hetz, J.M. Rollinger, A.A. Weissnicht, H. Stattner, Energy/temperature diagram and compression behavior of the polymorphs of D-mannitol, *J. Pharm. Sci.* 89 (2000) 457–468.
- [48] V. Vanhoorne, P.J. Van Bockstal, B. Van Snick, E. Peeters, T. Monteyne, P. Gomes, T. De Beer, J.P. Remon, C. Vervaet, Continuous manufacturing of delta mannitol by cospray drying with PVP, *Int. J. Pharm.* 501 (2016) 139–147.
- [49] N.Y. Chew, B.Y. Shekunov, H.H. Tong, A.H. Chow, C. Savage, J. Wu, H.K. Chan, Effect of amino acids on the dispersion of disodium cromoglycate powders, *J. Pharm. Sci.* 94 (2005) 2289–2300.
- [50] S.Schüle, T. Schulz-Fadembrecht, P. Garidel, K. Bechtold-Peters, W. Frieß, Stabilisation of IgG1 in spray-dried powders for inhalation, *Eur. J. Pharm. Biopharm.* 69 (2009) 793–807.
- [51] P. Lebrun, F. Krier, J. Mantanus, H. Grohgan, M. Yang, E. Rozet, B. Boulanger, B. Evrard, J. Rantanen, P. Hubert, Design space approach in the optimization of the spray-drying process, *Eur. J. Pharm. Biopharm.* 80 (2012) 226–234.
- [52] European Pharmacopoeia, 8<sup>th</sup> ed., EDQM, Council of Europe, Strasbourg, France, July 2013.
- [53] X. Li, F.G. Vogt, D. Hayes, H.M. Mansour, Design, characterization, and aerosol dispersion performance modeling of advanced co-spray dried antibiotics with mannitol as respirable microparticles/nanoparticles for targeted pulmonary delivery as dry powder inhalers, *J. Pharm. Sci.* 103 (2014) 2937–2949.
- [54] J. Lee, J.Y. Choi, C.H. Park, Characteristics of polymers enabling nano-comminution of water-insoluble drugs, *Int. J. Pharm.* 355 (2008) 328–336.
- [55] M. George, I. Ghosh, Identifying the correlation between drug/stabilizer properties and critical quality attributes (CQAs) of nanosuspension formulation prepared by wet media milling technology, *Eur. J. Pharm. Sci.* 48 (2013) 142–52.

## Tables

**Table 1** Matrix of full factorial design, yield of process and characteristics of spray-dried nanoparticle agglomerates: volume diameter, redispersibility (RDI %), fine particle fraction (FPF%) and fine particle dose (FPD).

**Table 2** Summary of the regression analysis and ANOVA results.

**Table 3** Nominal content and assayed ibuprofen content (% w/w) of nanoparticle agglomerates together with calculated drug loading efficiency (%) and residual moisture content (mean  $\pm$  SD, n=3).

**Table 1** Matrix of full factorial design, yield of process and characteristics of spray-dried nanoparticle agglomerates: volume diameter, redispersibility (RDI %), fine particle fraction (FPF%) and fine particle dose (FPD).

Formulation number	Pattern	Stabiliser	Mannitol to drug ratio	Leucine to drug ratio	Yield (%)	Volume diameter ( $\mu\text{m}$ )			RDI (%)	FPF (%)	FPD (mg)
						D10	D50	D90			
						1	100	HPMC			
2	200	TPGS	0.5	0.25	46.6	$0.85 \pm 0.01$	$6.20 \pm 0.05$	$9.02 \pm 0.13$	250	$46.62 \pm 5.6$	$4.42 \pm 0.7$
3	1++	HPMC	1	0.5	72.5	$0.85 \pm 0.00$	$3.57 \pm 0.03$	$6.82 \pm 0.07$	283	$68.55 \pm 3.8$	$6.23 \pm 0.6$
4	100	HPMC	0.5	0.25	56.4	$0.83 \pm 0.01$	$2.27 \pm 0.01$	$6.23 \pm 0.16$	400	$45.11 \pm 6.1$	$4.03 \pm 0.6$
5	2+-	TPGS	1	0	41.1	$1.13 \pm 0.05$	$9.88 \pm 0.39$	$24.39 \pm 2.70$	181	$9.32 \pm 2.5$	$0.79 \pm 0.3$
6	1-+	HPMC	0	0.5	60.1	$0.99 \pm 0.02$	$2.30 \pm 0.08$	$3.83 \pm 0.11$	751	$22.93 \pm 1.2$	$2.11 \pm 0.2$
7	2--	TPGS	0	0	27.3	$1.56 \pm 0.04$	$16.04 \pm 0.33$	$53.22 \pm 1.51$	765	$6.68 \pm 2.7$	$0.58 \pm 0.2$
8	2-+	TPGS	0	0.5	53.8	$0.88 \pm 0.02$	$2.15 \pm 0.02$	$3.81 \pm 0.01$	600	$40.00 \pm 2.3$	$3.66 \pm 0.2$
9	1+-	HPMC	1	0	47.9	$1.02 \pm 0.06$	$3.22 \pm 0.04$	$5.92 \pm 0.34$	307	$29.56 \pm 3.4$	$2.61 \pm 0.5$
10	2++	TPGS	1	0.5	60.0	$0.77 \pm 0.01$	$2.23 \pm 0.04$	$6.21 \pm 0.01$	148	$43.63 \pm 4.1$	$4.23 \pm 0.6$
11	200	TPGS	0.5	0.25	43.2	$0.87 \pm 0.01$	$5.20 \pm 0.04$	$7.31 \pm 0.30$	280	$40.23 \pm 2.7$	$3.64 \pm 0.4$
12	1--	HPMC	0	0	37.7	$0.96 \pm 0.03$	$4.29 \pm 0.09$	$6.87 \pm 1.01$	938	$5.84 \pm 2.8$	$0.46 \pm 0.2$



**Table 2** Summary of the regression analysis and ANOVA results.

Term	Yield			D <sub>50</sub> (µm)			RDI (%)			FPF (%)		
	Estimate	Std Error	p-value	Estimate	Std Error	p-value	Estimate	Std Error	p-value	Estimate	Std Error	p-value
Intercept	50.4	0.71	<0.0001	5.03	0.37	<0.0001	443.59	33.74	<0.0001	31.27	2.57	<0.0001
<i>Main effects</i>												
X <sub>1</sub> : Stabiliser	5.07	0.71	<b>0.0008</b> ***	-1.92	0.37	<b>0.0033</b> **	72.93	33.74	0.0830	2.73	2.57	0.3366
X <sub>2</sub> : Mannitol to drug ratio	5.33	0.87	<b>0.0017</b> ***	-0.74	0.45	0.1617	-266.89	41.32	<b>0.0013</b> **	9.45	3.14	<b>0.0298</b> *
X <sub>3</sub> : Leucine to drug ratio	11.55	0.87	<b>&lt;0.0001</b> ***	-2.90	0.45	<b>0.0013</b> **	-51.14	41.31	0.2708	15.48	3.14	<b>0.0044</b> **
<i>Two-way interactions</i>												
X <sub>1</sub> *X <sub>2</sub>	0.33	0.87	0.7231	0.79	0.45	0.1400	-7.89	41.31	0.8561	7.87	3.14	0.0543
X <sub>1</sub> *X <sub>3</sub>	0.2	0.87	0.8267	2.49	0.45	<b>0.0026</b> **	-1.64	41.31	0.9699	-1.44	3.14	0.6649
X <sub>2</sub> *X <sub>3</sub>	-0.68	0.87	0.4714	1.07	0.45	0.0620	32.89	41.31	0.4129	2.84	3.14	0.4071
<i>ANOVA</i>												
Model			<b>0.0004</b> ***			<b>0.0028</b> **			<b>0.0181</b> ***			<b>0.0251</b> *
R <sup>2</sup>	0.98			0.96			0.91			0.89		
Adj R <sup>2</sup>	0.96			0.91			0.80			0.76		

\* p< 0.05, \*\* p< 0.01, \*\*\* p< 0.001

**Table 3** Nominal content and assayed ibuprofen content (% w/w) of nanoparticle agglomerates together with calculated drug loading efficiency (%) and residual moisture content (mean  $\pm$  SD, n=3).

Pattern	Content (% w/w)				Assayed IBU	Drug Loading Efficiency (%)	Residual Moisture Content (%)
	Nominal						
	IBU	STAB	MAN	LEU			
<b>100</b>	54.05	5.41	27.03	13.51	50.8 $\pm$ 1.3	94.0 $\pm$ 2.4	3.5 $\pm$ 0.5
<b>200</b>	54.05	5.41	27.03	13.51	51.8 $\pm$ 1.7	95.9 $\pm$ 3.2	1.1 $\pm$ 0.2
<b>1++</b>	38.46	3.85	38.46	19.23	36.7 $\pm$ 0.2	95.4 $\pm$ 0.5	2.3 $\pm$ 0.4
<b>100</b>	54.05	5.41	27.03	13.51	49.2 $\pm$ 1.3	91.0 $\pm$ 2.6	3.0 $\pm$ 0.4
<b>2+-</b>	47.6	4.76	47.6	-	44.4 $\pm$ 0.8	93.2 $\pm$ 1.7	1.6 $\pm$ 0.1
<b>1-+</b>	62.5	6.25	-	31.25	59.4 $\pm$ 1.2	95.0 $\pm$ 1.8	3.4 $\pm$ 0.5
<b>2--</b>	91	9	-	-	77.4 $\pm$ 1.4	85.1 $\pm$ 1.6	2.3 $\pm$ 0.5
<b>2-+</b>	62.5	6.25	-	31.25	58.3 $\pm$ 1.1	93.3 $\pm$ 2.1	1.9 $\pm$ 0.1
<b>1+-</b>	47.6	4.76	47.6	-	42.1 $\pm$ 2.1	88.5 $\pm$ 3.6	2.7 $\pm$ 0.2
<b>2++</b>	38.46	3.85	38.46	19.23	35.4 $\pm$ 0.7	92.0 $\pm$ 1.9	1.6 $\pm$ 0.3
<b>200</b>	54.05	5.41	27.03	13.51	50.4 $\pm$ 2.1	93.2 $\pm$ 3.5	1.3 $\pm$ 0.3
<b>1--</b>	91	9	-	-	80.3 $\pm$ 1.9	88.2 $\pm$ 2.6	4.7 $\pm$ 0.4

## Figures

Figure 1 The three-dimensional design space of the  $2^3$  full factorial design.

Figure 2 z-average size and polydispersity index (PI) of ibuprofen nanosuspensions with increasing wet-milling time (mean + SD, n=3).

Figure 3 SEM image of ibuprofen starting material.

Figure 4 SEM images of ibuprofen nanoparticle agglomerates included in the full factorial design. The stabiliser is HPMC.

Figure 5 SEM images of ibuprofen nanoparticle agglomerates included in the full factorial design. The stabiliser is TPGS.

Figure 6 Surface plots indicating the effect of mannitol to drug ratio and leucine to drug ratio on the yield and  $D_{50}$  particle size of the nanoparticle agglomerates stabilised with HPMC (a,c) and TPGS (b,d). The arrows indicate the direction of increasing values of the variables.

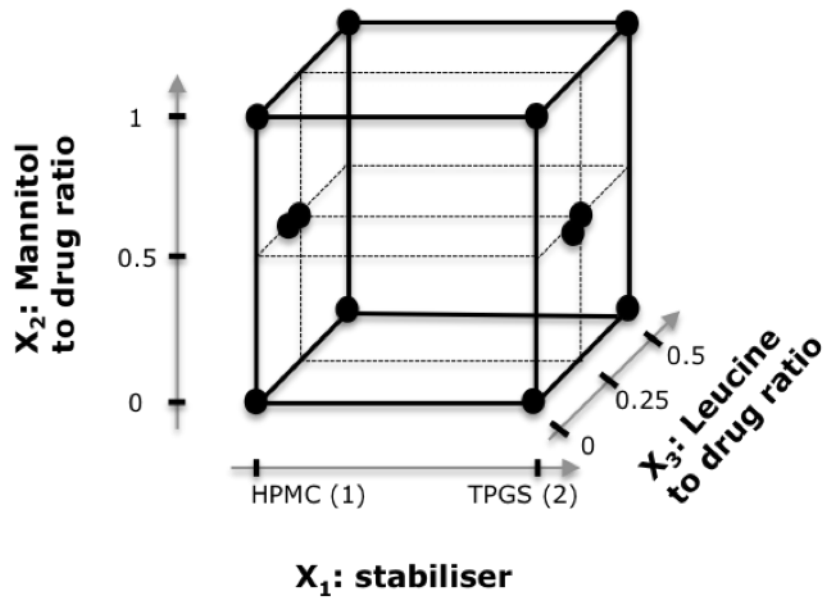
Figure 7 Surface plots indicating the effect of mannitol to drug ratio and leucine to drug ratio on the redispersibility and the FPF% of the nanoparticle agglomerates stabilised with HPMC (a,c) and TPGS (b,d). The arrows indicate the direction of increasing values of the variables.

Figure 8 XRPD diffractograms of (a) starting materials and (b) nanoparticle agglomerates included in the full factorial design.

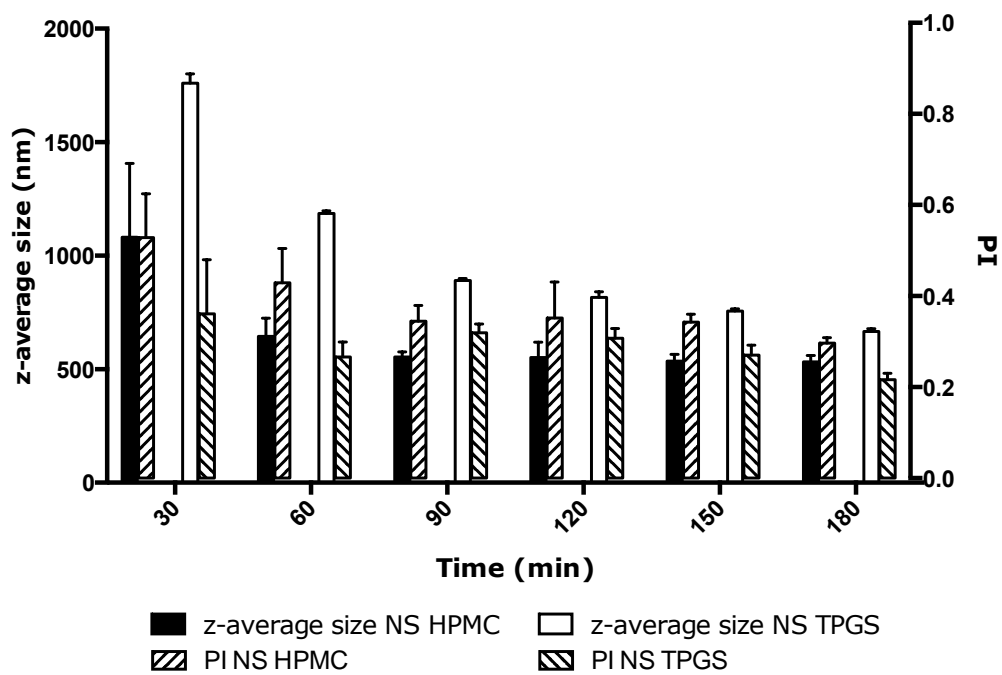
Figure 9 DSC thermograms of (a) ibuprofen and mannitol starting materials and (b) nanoparticle agglomerates included in the full factorial design. A magnified thermogram between 130 °C and 170 °C, for the pattern 1++, is given in the insert.

Figure 10 Dissolution profiles of ibuprofen starting material and nanoparticle agglomerates included in the full factorial design (mean + SD, n=3). The stabiliser is (a) HPMC and (b) TPGS.





**Figure 1** The three-dimensional design space of the  $2^3$  full factorial design.



**Figure 2** z-average size and polydispersity index (PI) of ibuprofen nanosuspensions with increasing wet-milling time (mean + SD, n=3).

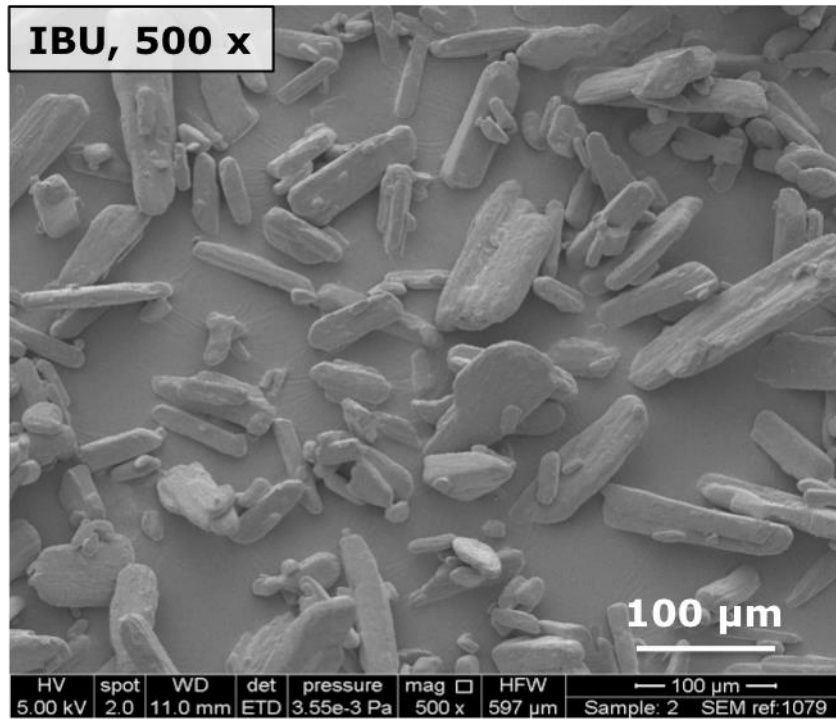


**Figure 3** SEM image of ibuprofen starting material.

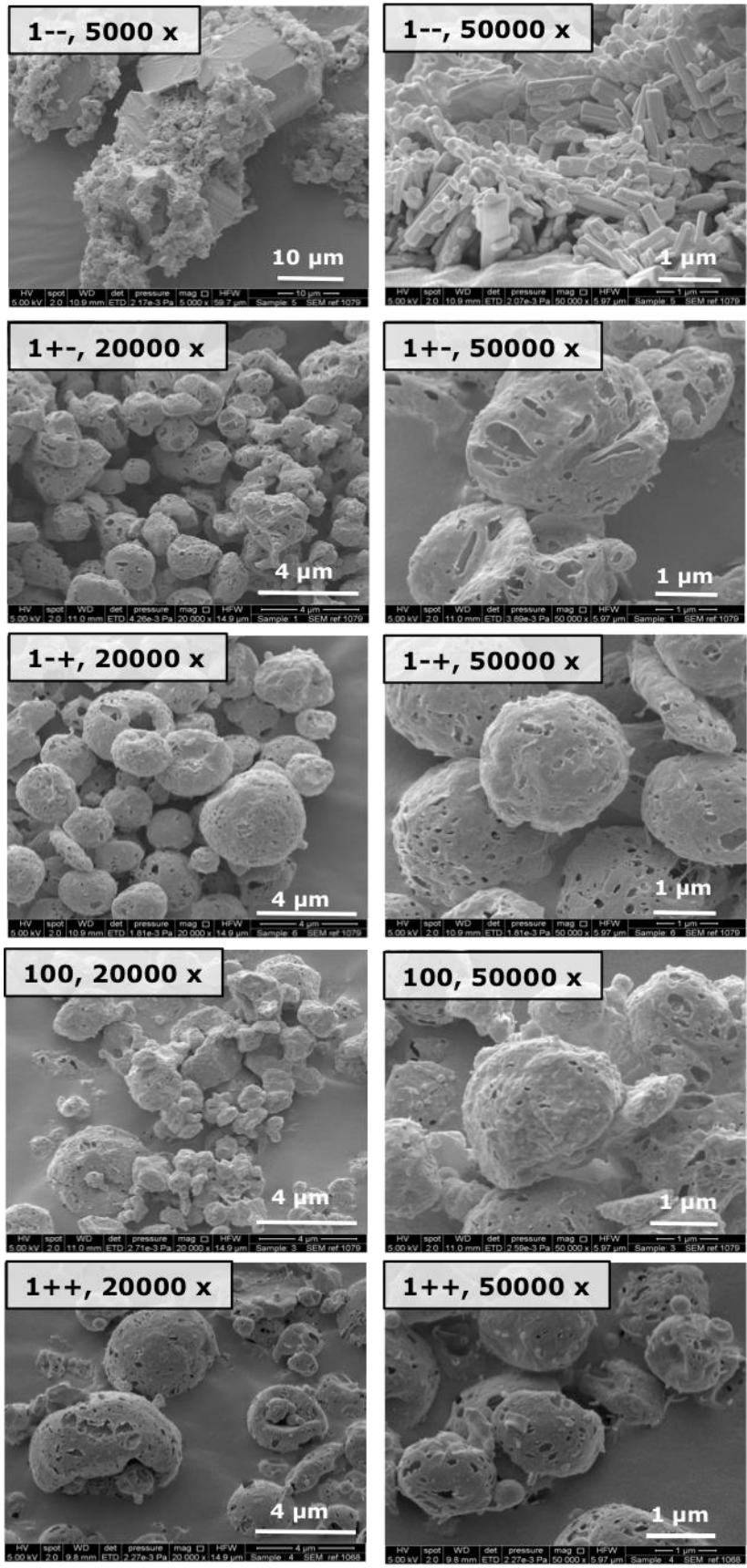


**Figure 4** SEM images of ibuprofen nanoparticle agglomerates included in the full factorial design. The stabiliser is HPMC.

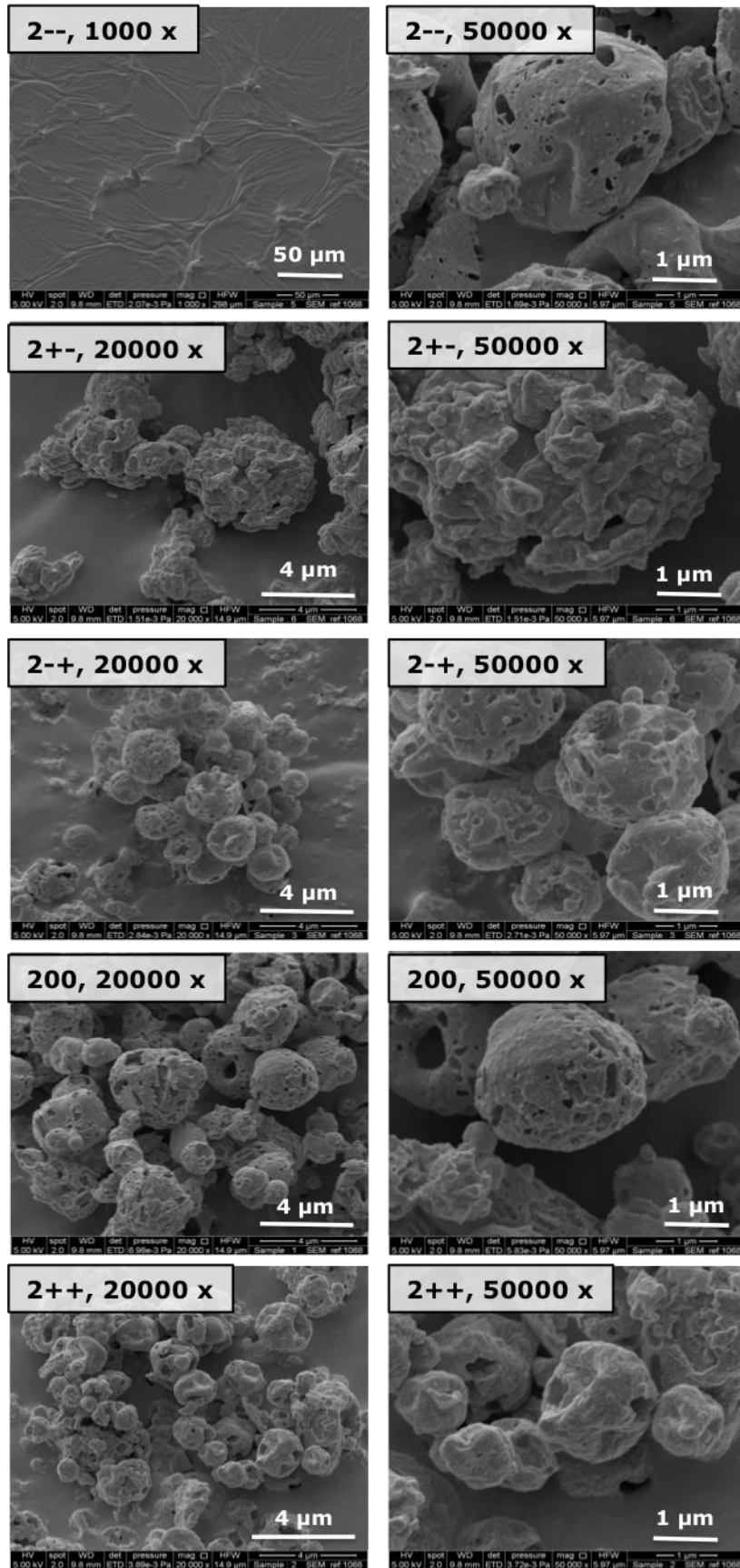


**Figure 5** SEM images of ibuprofen nanoparticle agglomerates included in the full factorial design. The stabiliser is TPGS.

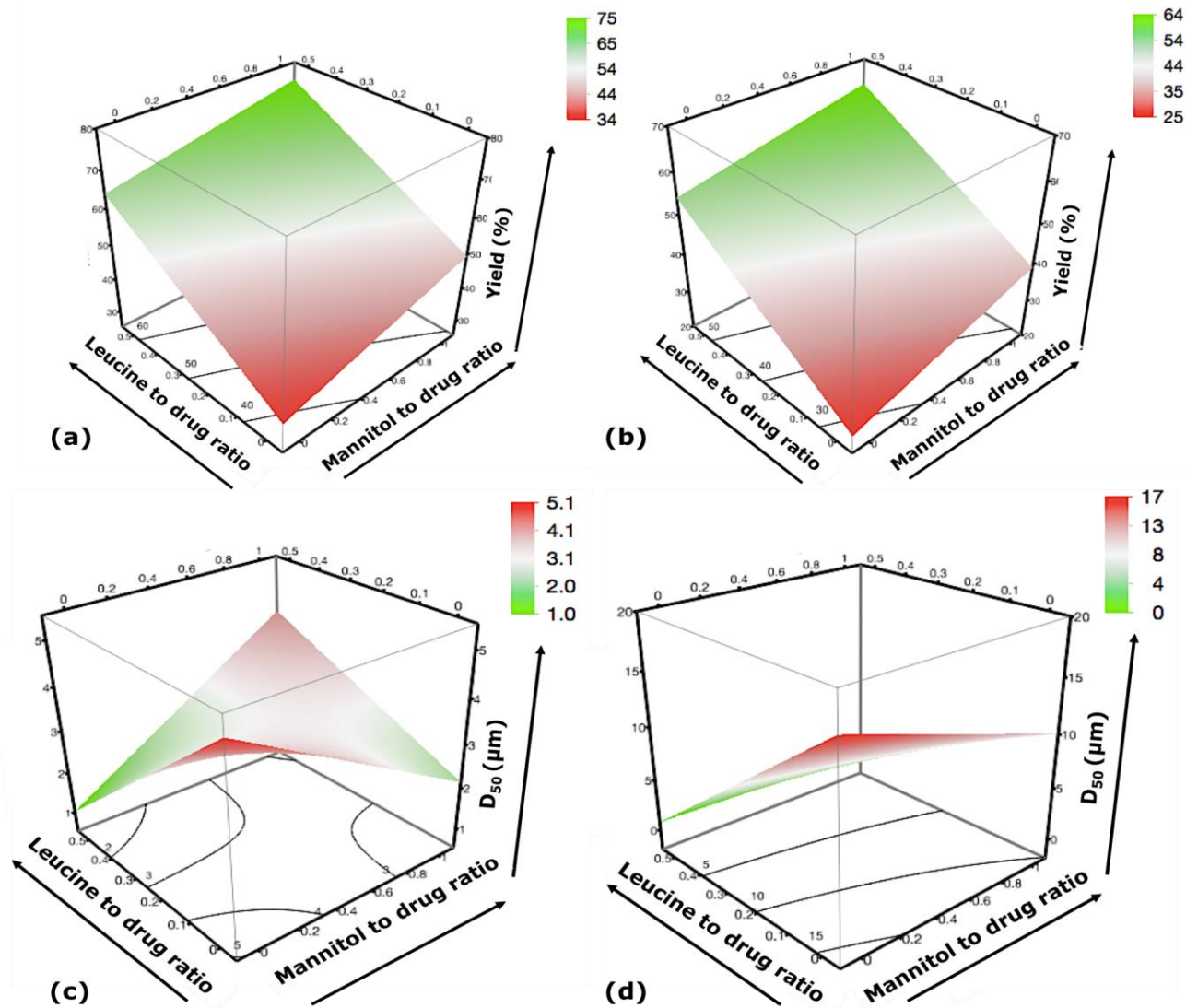


**Figure 6** Surface plots indicating the effect of mannitol to drug ratio and leucine to drug ratio on the yield and  $D_{50}$  particle size of the nanoparticle agglomerates stabilised with HPMC (a,c) and TPGS (b,d). The arrows indicate the direction of increasing values of the variables.

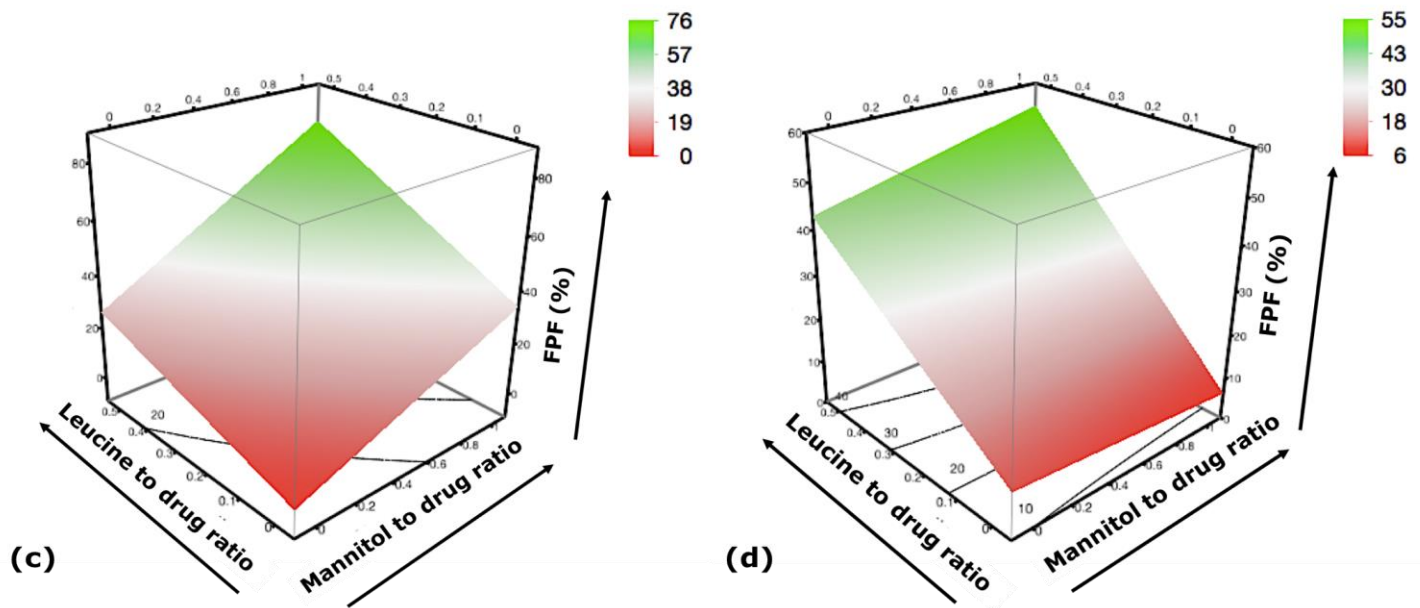
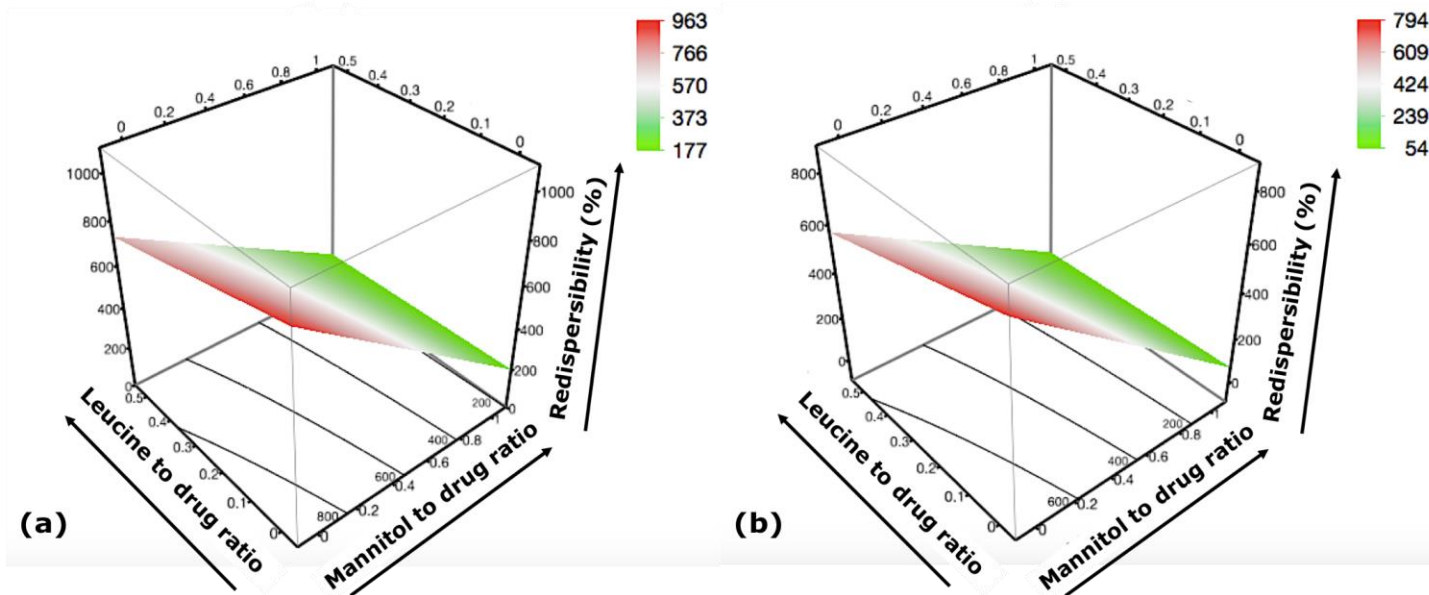


**Figure 7** Surface plots indicating the effect of mannitol to drug ratio and leucine to drug ratio on the redispersibility and the FPF% of the nanoparticle agglomerates stabilised with HPMC (a,c) and TPGS (b,d). The arrows indicate the direction of increasing values of the variables.



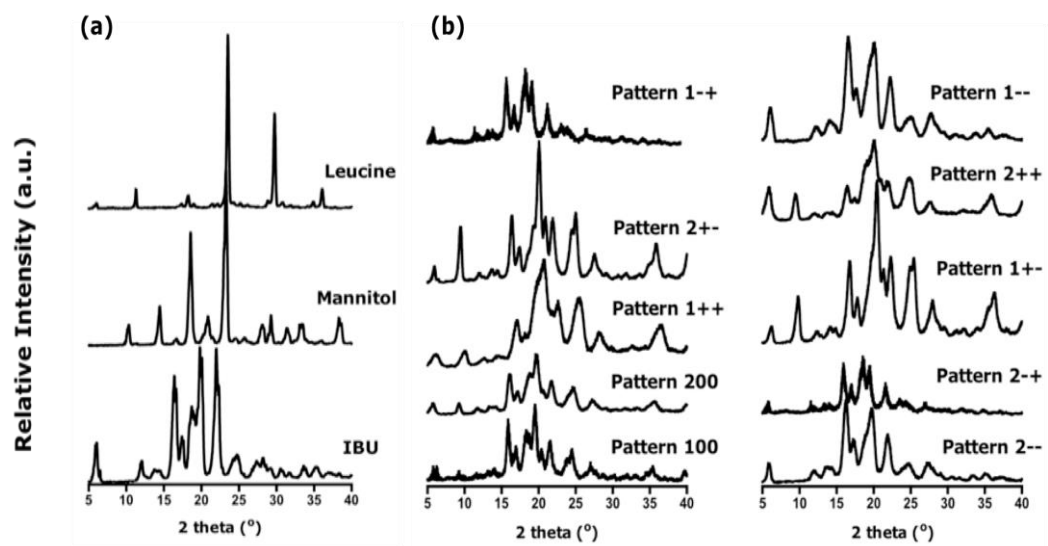


**Figure 8** XRPD diffractograms of (a) starting materials and (b) nanoparticle agglomerates included in the full factorial design.

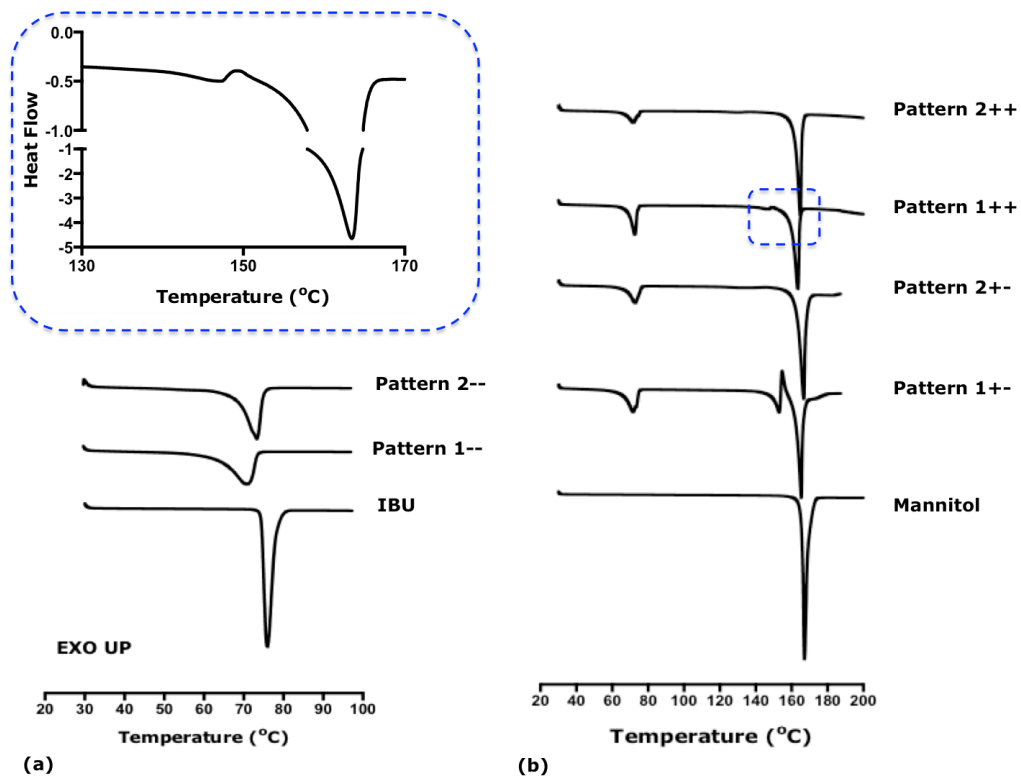
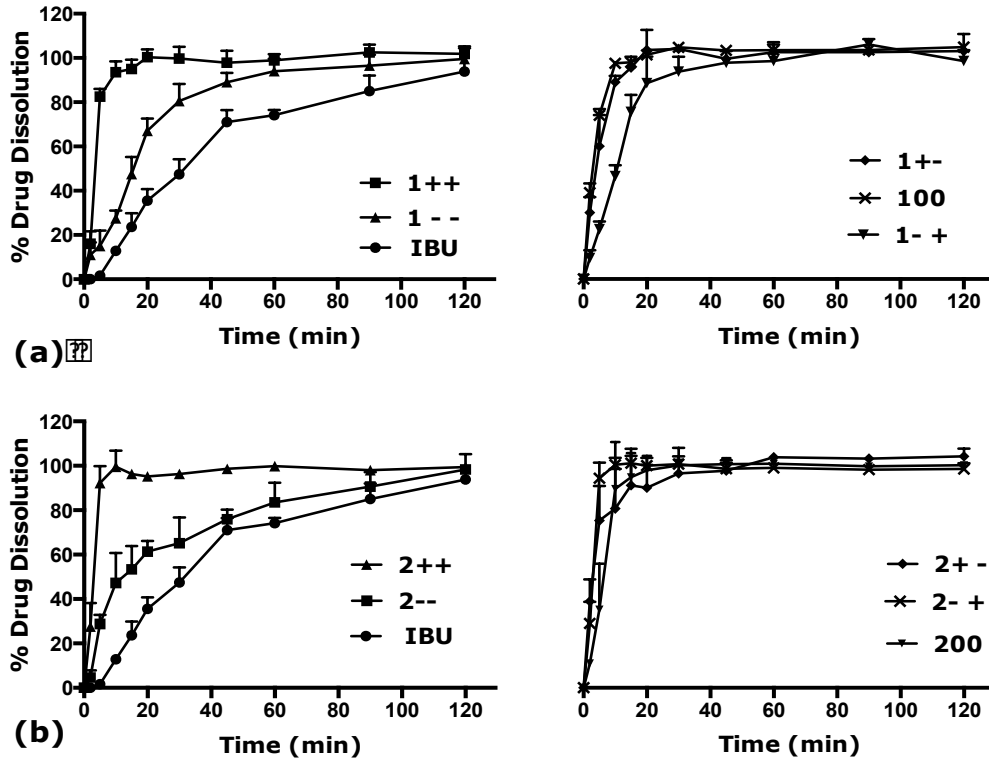


**Figure 9** DSC thermograms of (a) ibuprofen and mannitol starting materials and (b) nanoparticle agglomerates included in the full factorial design. A magnified thermogram between 130 °C and 170 °C, for the pattern 1++, is given in the insert.



1

2 **Figure 10** Dissolution profiles of ibuprofen starting material and nanoparticle  
 3 agglomerates included in the full factorial design (mean + SD, n=3). The stabiliser  
 4 is (a) HPMC and (b) TPGS.

5